RSC Advances

ROYAL SOCIETY OF CHEMISTRY

www.rsc.org/advances

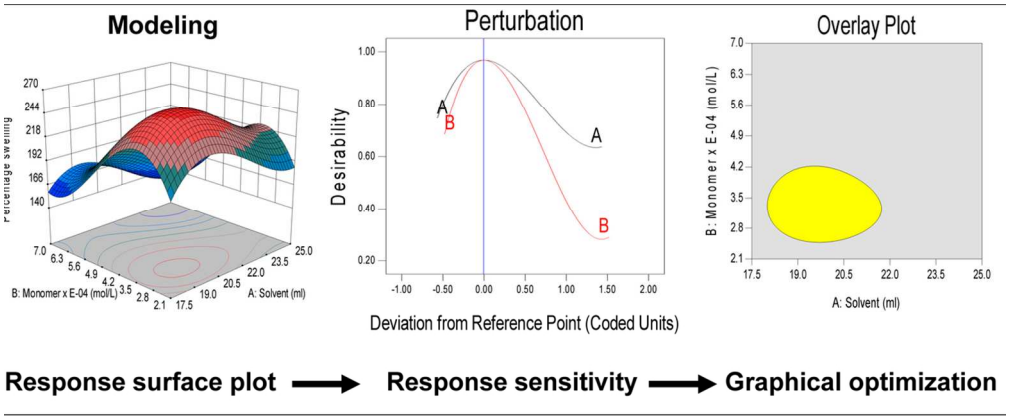

114x46mm (300 x 300 DPI)

Optimal response surface design of Gum tragacanth based poly[(acrylic acid)-co-acrylamide] IPN hydrogel for controlled release of antihypertensive drug losartan potassium

Balbir S. Kaith [1]*, Saruchi Sharma [1], Rajeev K. Jindal [1], Vineet Kumar [2] and Manpreet S. Bhatti [3]

[1] Department of Chemistry, Dr. B.R. Ambedkar National Institute of Technology, Jalandhar, Punjab, India Email: bskaith@yahoo.co.in

[2] Department of Chemistry, CT Institutions, Jalandhar, Punjab, India

[3] Department of Botanical and Environmental Sciences, Guru Nanak Dev University, Amritsar, Punjab, India Email: mbhatti73@gmail.com

Corresponding author:

Dr. Balbir S Kaith,
Professor,
Department of Chemistry,
Dr. B.R. Ambedkar National Institute of Technology,
Jalandhar, Punjab, India
Email: bskaith@yahoo.co.in
Phone: 91-9780684883

Abstract

The present study envisaged the development and optimization of new interpenetrating polymer network (IPN) constituting of *Gum tragacanth*, poly(acrylic acid) (PAA) and poly(acrylamide) (PAAm) for *in situ* controlled release of losartan potassium under different pH conditions at 37^0C. Amount of Solvent and monomer concentration were chosen as process variables and percentage swelling was taken as a response. The ANOVA model fits into the data and gave cubic model as best fit with predicted R^2 = 0.976. The maximum desirability of achieving the goal was observed to be 19.63 ml solvent and 3.28 x 10^{-4} mol/L monomer concentration at which percentage swelling was found to be 266. Whereas, at 23.7 ml solvent and 6.7 x 10^{-4} mol/L monomer, the percentage swelling was found to be minimum (139%). The model was validated at the optimal points for developing of device with maximum swelling capacity. Drug release through the synthesized matrix was found to show non-fickian behave at pH 2.0, 7.0 and 9.2with increasing trend in gel characterstic constant (k). At each pH medium initial diffusion constant (D_I) has been found to be higher than lateral diffusion constant (D_L)

Keywords: Carbohydrate biopolymer; Antihypertensive drug**;** Hydrogel; Modelling; Response surface methodology (RSM); Controlled drug delivery

1. INTRODUCTION

Attention of researchers all over the world has been focused on the design and development of multipolymer devices because of their better performance compared to that of individual components. Since homopolymer and copolymer hydrogels alone cannot meet out the divergent demands both in properties and performances, therefore, an Interpenetrating polymer networks (IPN) system is better approach. IPNs comprised of two or more than two polymer networks that are formed in the presence of one another, have been found to be the versatile suitable materials for biomedical applications. Many IPNs are prepared from water soluble polymers through cross-linking using chemical or enzymatic initiators (1-5). Different properties of IPN- system like porocity, elasticity and response to external stimuli can be tuned with respect to types of cross-linking agents and their proportions.

Since IPNs are capable of delivering drugs at constant rate for specific time intervals, therefore, scientists are using them as devices for controlled drug delivery. Such devices are also used in tissue engineering field as scaffolds (6). Ekici and Saraydin prepared IPN hydrogel based on chitosan, poly(N-vinyl pyrrolidene) and poly(acrylic acid) for the gastrointestinal release of amoxicillin (7). PAAc-based hydrogels are investigated as a device for bioadhesive release and Ag/P(HEMA/IA)/PVP interpenetrating network has been used as an antimicrobial agent (8,9).

Gum tragacanth is a gummy exudation obtained from shrubby locoweeds in the native region of the Eastern Mediterranean and South Western Asia. Iran is the biggest producer of the *Gum tragacanth*. It is a carbohydrate biopolymer possessing molecular weight 8 40,000 g/mol and is comprised of two main fractions. One is tragacanthin and other is bassorin. On mixing with water, only soluble fraction called tragacanthin dissolves and gives colloidal hydrogel, while insoluble fraction bassorin swells to form gel (10-13).

Present work deals with the synthesis of new interpenetrating polymer network (IPN) consisting of *Gum tragacanth*, poly(acrylic acid) (PAA) and poly(acrylamide) (PAAm) using glutaraldehyde as the cross-linker. Two process variables (solvent and monomer) were varied as per IV-optimal design strategy of response surface

methodology (RSM). The maximizing percentage swelling was taken as response. ANOVA model was constructed which best fits the response data. Finally, desirability function and ramp functions were used for process optimization. The synthesized IPN contain hydrophilic chains. These hydrophilic chains help in easy loading and sustained release of the drug from the synthesized IPN. Thus, the synthesized IPN are the promising approach to achieve *in-vitro* buoyancy and it also improves the absorption of losartan potassium in the gastrointestinal tract for longer time, therefore, it was found to be a suitable device for controlled drug release. Thus, the synthesized IPN matrix was used for controlled release of antihypertensive drug losartan potassium (14, 15) under varying pH and time.

Interpenetrating polymer networks is better than some other hydrogels or drug delivery carriers because better performances of IPN over the conventional individual polymers and all class of materials. The superior properties of IPNs like swelling capacity, stability, biocompatibility, nontoxicity and biodegradability have attracted considerable attention in delivering bioactive molecules. In the last few years various research reports on the IPN based delivery systems showed that these carriers have emerged as a novel carrier in controlled drug delivery (24).

2. MATERIALS AND METHODS

Gum tragacanth, potassium persulphate and ascorbic acid were purchased from SD Fine Chemical Pvt. Ltd. Acrylic acid and acrylamide were obtained from Merck. The model drug losartan potassium was obtained from Cipla. All the above chemicals were of analytical grade and were used as received. Deionised water was used in carrying out all the reactions during experimentation.

FTIR spectra of *Gum tragacanth*, Gt-cl-poly(AA) [Gum tragacanth-crosslinked-poly(acrylic acid)] and Gt-cl-poly(AA-ip-AAm) [*Gum tragacanth*-poly(acrylic acid-co-acrylamide) interpenetrating polymer network] were recorded using Perkin Elmer spectrophotometer to determine their structures. Samples were thoroughly mixed with dried KBr and pellets were prepared by compression under vacuum. Scanning electron microscopy (SEM) of samples was taken on LEO-435VF, LEO Electron Microscopy Ltd. Drug release was studied using UV-VIS spectrophotometer (Double beam Systronic-2201) with sensitivity of 0.1 ppm and drug loading of 50 ppm.

2.1 Preparation of IPN

Gt-cl-poly(AA) were prepared by the method describe earlier (16) was suspended in the deionised water. Known concentration of acrylamide was added with continuous stirring and was kept overnight. To the reaction mixture ascorbic acid-potasium persulphate as an initiator and glutaraldehyde as a crosslinker were added with continuous stirring. Reaction was carried-out at specific temperature and time. Homopolymer was removed with aqueous extraction. Synthesized IPN was dried at 50^0C till constant weight was obtained. Concentration of acrylamide was optimized with respect to percentage swelling and was calculated using Eq. 1.

$$\text{Percentage swelling } (P_s) = (W_s - W_d) / W_d \times 100 \quad (1)$$

where, W_s and W_d are the weights of swollen and dry polymer, respectively.

2.2 Swelling Studies

Pre-weighed dry IPN sample was immersed in distilled water and after every 2 h interval, weight gained by the sample was noted down until equilibrium was attained. Swollen IPN sample was separated from the water by using mesh screen, drained on the sieve for 5 min until no redundant water was left behind. The percentage swelling of the synthesized IPN was calculated using Eq. (1).

2.3 Experimental design

RSM is an efficient technique for process optimization in minimum experimental run. In this manuscript, an IV optimal design was used. The design was used to minimize the integral of the prediction variance across the design space. These designs were built algorithmically using CONVERT algorithm to provide lower prediction variance across the entire design space. IV-optimal designs were the best used with response surface designs. With response surface designs the goal was to model the true response surface with greater precision. Lack-of-fit points were added to the design to fill the largest gaps by selecting a group of points that could maximize the minimum distance to another point. Similarly, replicates were chosen that could best support the optimality criterion along with additional center points. There were two process variables and one response variable along with the range given in Table 1. There were total of 22 runs as given in Table 2, which included six

model points, five runs were used to estimate *lack of fit*, four replicates at center point and additional seven runs at edges and vertices.

2.4 Drug loading and release studies

There are two methods of drug loading onto IPN matrix. In one method, drug is mixed with the monomer followed by initiator, with or without cross-linking agent and allowed to polymerize. This method entraps the drug within the matrix. Whereas in the second method, gel is swelled in the drug solutions until equilibrium is attained followed by drying to obtain the release device. The second method of drug imbibing has certain advantages over the first as the polymerization conditions may have adverse effect on drug properties. It may also cause difficulty in device purification. In the present work, second method of drug loading was followed. Solution containing 2 g/L of drug was prepared in distilled water. λ_{max} was noted and calibration curve was prepared for absorbance *vs.* drug concentration. The drug loaded IPN was placed in different pH media to carrying out drug release behavior. All drug release experiments were carried out at 37°C. The concentration of the losartan potassium released was taken after every two hours time interval. This was followed by the drug release kinetics with respect to pH and time. UV-Vis spectrophotometer (Double beam Systronic-2201) was used for the evaluation of drug release through the synthesized IPN.

2.5 Mathematical analysis of drug release behavior

Mathematical model was used to study the drug release behavior through synthesized IPN. Liquid uptake i.e. weight gain (Ms) was evaluated using Eq. (2).

$$M_s = kt^n \quad (2)$$

where 'k' is gel characteristic constant, 'n' is diffusion exponent. n = 0.5 revealed the normal fickian diffusion, if the value of 'n' lies between 0.5 to 1, it signifies anomalous or non-fickian diffusion. However if n >1, then it signifies Case II diffusion. Fick's power law Eq. (3) was used to evaluate the drug release through the IPN (15,18).

$$M_t/M_\infty = kt^n \quad (3)$$

where, M_t is the fractional release of the drug at different time interval, M_∞ is the fractional release of the drug at equilibrium. This equation could be applied for the

60% release of the drug. The value of ‘’n and ‘k’ are obtained from the slope and intercept of the plot between M_t/M_∞ versus lnt.

2.6 Diffusion exponent of the drug release

Ficks law was used to describe the diffusion process (19-23). Initial diffusion coefficient (D_I) was calculated using Eq. (4).

$$M_t/M_\infty = 4 \times D_i/\pi l^2 \quad (4)$$

where, M_t/M_∞ is the fractional release of the drug. M_t and M_∞ are the drug release at time t and at equilibrium, respectively. L is the thickness of the IPN sample used.

Average diffusion coefficient (D_A) was calculated from the following Eq. (5).

$$D_A = 0.049l^2/t^{1/2} \quad (5)$$

where, $t_{1/2}$ is the time required for 50% release of the drug.

Lateral diffusion coefficient (D_L) was calculated using the Eq. (6).

$$M_t/M_\infty = 1- (8/\pi^2) \exp(-\pi^2 Dt/l^2) \quad (6)$$

D_L was also evaluated using the slope of the plot between $\ln(1-M_t/M_{oo})$ *vs.* time as per Eq. (7).

$$D_L= (\text{slope } l^2/8) \quad (7)$$

3. RESULTS AND DISCUSSION

3.1 RSM Modeling

The experimental design along with the actual response data is given in Table 2. ANOVA sequential model sum of squares proposed cubic model as best fit models. Although, quadratic model have explained good model variance (Adjusted R^2>0.8), but model *lack of fit* was found to be significant. This indicated that model noise was more than signal and model can not be navigated in the design space. Whereas, cubic model was highly significant (Adjusted R^2=0.984, F-value=144) with non significant *lack of fit* (p=0.253 at F=1.61). Looking at individual model terms, few model terms were non-significant at p-value greater than 0.05. Thus, model was again generated after eliminating non significant model terms. The reduced cubic model again significant at F=173 with *lack of fit* not-significant (p=0.355). The

model statistics like coefficient of variation (CV) of 2.14% and predicted R^2=0.976 was closed to adjusted R^2 =0.985 indicated about excellent model fitting. Also, signal to noise (S/N) ratio of 44.6 indicated that model noise is not-significant as compared to signal. Thus, model could be navigated in the design space. The unit-less regression equation in terms of coded factors is given in Eq. (8) and in terms of actual factors in Eq. (9). The results of ANOVA statistics are given in Table 3.

$$Ps= 227.81- 42.81\ A - 87.49\ B - 1.34\ A \times B - 22.07\ A^2 - 35.09\ B^2 + 6.30\ A^2 B + 35.76\ A^3 + 60.23\ B^3 \quad (8)$$

where Ps= Percentage swelling; A: solvent and B: Monomer are in coded units.

$$Ps = - 7484 + 1010\ A + 360\ B - 7.93\ A \times B - 45.63\ A^2 - 62.17\ B^2 + 0.183\ A^2 B + 0.678\ A^3 + 4.12\ B^3 \quad (9)$$

where Ps= Percentage swelling; A: solvent is in ml and B: Monomer x 10^{-4} is in mol/L.

Before moving to the response surface plots, diagnostic statistics were studied using normal plot of residuals to satisfy the normal distribution of error as given in Fig. 1a. The actual *vs.* predicted response plot for percentage swelling is given in Fig. 1b

The response plots were generated using regression equations. Percentage swelling is taken as response and solvent and monomer concentration is varied in the designed space. The maximum percentage swelling was obtained in the solvent range of 19 to 20 ml. Similarly, monomer was in the range of 2.8 x 10^{-4} to 3.5 x 10^{-4} mol/L to get maximum percentage swelling (Fig. 2). Whereas, minimum percentage swelling was obtained when, maximum amount of solvent is added (25 ml) with maximum amount of monomer addition (7 x 10^{-4} mol/L). This indirectly indicated that solvent and monomer has weak interaction and may be interacting either through higher terms.

3.2 Process optimization

Numerical optimization was achieved through perturbation plot and desirability plot. The independent variables were set within the range and percentage swelling was set as maximize. Through random sampling point, best process conditions were achieved at 19.63 ml solvent and 3.28 x 10^{-4} mol/L monomer (Table 4). The

maximum percentage swelling achieved at optimized conditions was found to be 266. The results were verified by validation testing at new proposed conditions. Using experimental design optimization, there was approximately 92% increase in percentage swelling (140 to 270) depicted through desirability plot (Fig. 3a). The perturbation plot helped to compare the response sensitivity at the optimized conditions. In this, one variable was found to change while other holding constant at optimized conditions. A higher slope or curvature in a factor shows response sensitivity. Monomer was more sensitive than solvent at optimized conditions (Fig. 3a). Graphical optimization commonly known as overlay plot was studied. The central elliptical (yellow) area represents those process conditions at which minimum percentage swelling was 250. To achieve minimum percentage swelling of 250, solvent should range between 18 to 21.69 ml and monomer concentration between 2.4 x 10^{-4} to 4.2 x 10^{-4} mol/L (Fig. 3b).

3.3 Characterization studies

3.3.1 FT-IR Spectroscopy

In case of *Gum tragacanth*, broad peaks obtained were 3427.08 cm^{-1} (due to O-H stretching of the carbohydrate e), 2934.78 cm^{-1} (CH_2 asymmetric stretching),1039.07 cm^{-1} (C-O stretching region as complex bands, resulting from C-O and C-O-C stretching vibrations) and 638 cm^{-1} was (due to pyranose ring). In case of Gt-cl-poly(AA), additional peaks were obtained at 1750.23 cm^{-1} and 1613.40 cm^{-1} were due to C=O stretching in carboxylic acid. Peaks at 2854.31cm^{-1}, 2659.42 cm^{-1} and 2521.73 cm^{-1} were due to O-H stretching of the carboxylic acid, while in case of Gt-cl-poly(AA-ip-AAm) peaks near 1450 cm^{-1} was due to $–NH_2$ plane bending of the amide II band. Peaks at 1200 and 1600 cm^{-1} were due to –C-N stretching of the amide III band and –C=O stretching of the amide I band, respectively (Fig. 4).

3.3.2 SEM

Gum tragacanth, Gt-cl-poly(AA) and Gt-cl-poly(AA-ip-AAm) were morphologically examined with the help of scanning electron micrographs (SEM). Samples were gold plated in order to have good conductive effect. SEM of *Gum tragacanth* showed no deposition of poly(monomeric) chains and is without any type of cross-linking (Fig. 5a). Whereas, SEM of Gt-cl-poly(AA) revealed the cross-

linking between the –OH groups of polysaccharide chains of backbone and poly(AA) chains through glutaraldehyde linkage (Fig. 5b). However, introduction of poly(AAm) chains in between the poly(AA) grafted polysaccharide chains entered into physical and chemical interaction between poly(AA) grafted polysaccharide chains and poly(AAm) chains resulting in the formation of IPN system. Comparison of the scanning electron micrograph of *Gum tragacanth*, Gt-cl-poly(AA) and Gt-cl-poly(AA-ip-AAm) revealed a clear cut distinction between them (Figs. 5a-c).

3.4 Drug release at varying pH and time

Losartan Potassium was selected as a model drug. Drug loading efficiency of the synthesized IPN was found to be 79%. The synthesized IPN contain hydrophilic chains. These chains helps in easy slipping of the drug molecules in the synthesized IPN matrix and thus leads to the easy loading of the drug into the matrix. These groups also help in the easy dissolution as well as easy diffusion of the drug through the matrix. Synthesized IPN hydrogel was found to swell constantly as a function of time, so it was found suitable device for controlled release of drug. Various pH solutions 2.0, 7.0 and 9.2 were used as releasing media. The drug release behavior was studied at different pH. It has been found from the result that initial release of losartan potassium was 40.56 ppm at 2 hour time interval (D_I= 4.523, pH= 7.0) followed by 41.67 ppm at 2.0 pH (D_I= 4.441) and 52.4 ppm at pH 9.2 (D_I=6.547). However final release of the drug occurred after 34 h was found to be maximum in alkaline medium (D_L= 1.98, pH= 9.2) and minimum in neutral medium Table 5. The drug release was found to increase with increase in pH, this was due to the fact that –COOH groups on the polymeric chain are in unionized form at lower pH, resulting in the collapsed state of the IPN hydrogel matrix. The drug release rate was little bit higher at higher pH because these groups get partially ionized to $–COO^-$. These ionic charges repel each other leading to increased drug diffusion from the device. The drug release was also found to be dependent on time. Initially the drug release was slow but it kept on increasing with the passage of time and after reaching the maximal, equilibrium was attained with constant release of losartan potassium (Fig. 6). This could be due to the fact that in the initial stage the drug loaded polymer matrix swell slowly under different pH media, which allow slow diffusion of the drug, which further increase with time until equilibrium was attained.

4. CONCLUSIONS

Response surface methodology is an effective experimental design tool for maximizing drug uptake capacity. Novel interpenetrating polymeric network (IPN) was successfully synthesized and was found to possess desired swelling capacity. The IPN was found to be pH sensitive towards the controlled release of antihypertensive drug losartan potassium. The final release of the drug from the matrix occurred after 34 h, which indicated that the synthesized device could be used as a drug carrier for prolonged release of losartan potassium.

ACKNOWLEDGMENTS

The financial support by Ministry of Human Resource Development, New Delhi for providing fellowship (No. F. 9-2/2007 TS.I) to Suruchi Sharma is acknowledged.

REFERENCES

1. Wang, W., & Wang, A. (2010). Synthesis and swelling properties of pH-sensitive semi-IPN superabsorbent hydrogels based on sodium alginate-g-poly(sodium acrylate) and Polyvinylpyrrolidone. *Carbohydrate Polymers,* 80**,** 1028–1036.
2. Hua, S. B., & Wang, A. Q. (2009). Synthesis, characterization and swelling behaviors of sodium alginate-g-poly(acrylic acid)/sodium humate superabsorbent. *Carbohydrate Polymers***,** 75**,** 79–84.
3. Jin, S. P., Liu, M. Z., Zhang, F., Chen, S. L., & Niu, A. Z. (2006). Synthesis and characterization of pH-sensitivity semi-IPN hydrogel based on hydrogen bond between poly(N-vinylpyrrolidone) and poly(acrylic acid). *Polymer,* 47**,** 1526–1532
4. Kabiri, K., Omidian, H., Hashemi, S. A., & Zohuriaan-Mehr M. J. (2003). Synthesis of fast-swelling superabsorbent hydrogels: effect of crosslinker type and concentration on porosity and absorption rate. *European Polymer Journal* **,** 39**,** 1341–1348.
5. Wang, W., Wang, Q., & Wang, A. (2011). pH-responsive carboxymethylcellulose-g-poly(sodium acrylate)/polyvinylpyrrolidone semi-IPN hydrogels with enhanced responsive and swelling properties. *Macromolecular Research***,** 19**,** 57-65.

6. Bajpai, A. K., & Mishra, A. (2008). Carboxymethyl cellulose (CMC) based semi-IPNs as carrier for controlled release of ciprofloxacin: an in-vitro dynamic study. *J. Mater Sci: Mater. Med.*, 19**,** 1221-1230.
7. Ekici, S., & Saraydin, D. (2007) Interpenetrating polymeric network hydrogels for potential gastrointestinal drug release. *Polymer International***,** 56**,** 1371-1377.
8. Jovasevic, J. S., Dimitrijevic, S. I., Filipovic, J. M., Tomic, S. L., Micicand, M. M., & Suljovrujic, E. H. (2011). Swelling, Mechanical and Antimicrobial Studies of Ag/P(HEMA/IA)/PVP Semi-IPN Hybrid Hydrogels. *Acta Physica Polonica***,** 120**,** 279-283.
9. Chen, J., Yang, L., Wu, M., Xi, Q., He, S., Li, Y., & Nho, Y.C. (2000). Preparation of interpenetrating polymer networks by two times grafting of monomers onto preirradiated polypropylene ®lm. *Radiation Physics and Chemistry***.** 59**,** 313-316.
10. Kabiri, K., & Nouri, M. R. (2008). Tragacanth gum-graft-polyacrylonitrile: synthesis, characterization and hydrolysis. *J. Polym. Res.*, 15**,** 173-180.
11. Khajavi, R., Pourgharbi, S. H. M., Kiumarsi, A., & Rashidi, A. (2007). Gum tragacanth fibers from Astragalus gummifer species: Effects of influencing factors on mechanical properties of fibers. *J. Applied Sci***.,** 7**,** 2861-2865.
12. Balaghi, S., & Mohammadifar, M. A. (2010). Physiochemical and rheological characterization of Gum tragacanth exudates from six species of Iranian Astragalus Food. *Biophysics***,** 5**,** 59-71.
13. Weiping, W. Branwell, A., & Essex, C.L. (2000). Tragacanth and karaya. Woodhead Publishing Limited and CRC Press LLC.
14. Avulapati, S., Roy, A. K., Shashidhar, K. R., Reddy, T., & Reddy, U. (2011). Formulation And Evaluation Of Taste Masked And Fast Disintegrating Losartan Potassium Tablets. *International Journal of Drug Development & Research***,** 3, ISSN 0975-9344.
15. Patil, P. R., Rakesh, S. U., Dhabale, P. N., & Burade, K. B. (2009). RP- HPLC method for simultaneous estimation of losartan potassium and amlodipine besylate in tablet formulation. *International Journal of Chem. Tech. Research CODEN(USA),* **1,** 464-469.

16. Kaith, B. S., Saruchi, Jindal, R., & Bhatti, M.S. (2012). Screening and RSM optimization for synthesis of *Gum tragacanth*-acrylic acid based device for *in-situ* controlled cetirizine dihydrochloride release. *Soft Matter***,** 8**,** 2286-2293.
17. Baba, M., Puisieux, F., Marty, J. P.,& Carstensen, J. T. (1979). Physical mode for release of drug from gel forming sustained release preparations. *Int. J. Pharma***,** 979**,** 3, 87-92.
18. Alfrey, T., Gurnee, J. E. F., & Lloyd, W. G. (1966). Diffusion in glassy polymers. *Journal of Polymer Science: Part C***,** 249-261.
19. Saruchi, Kaith, B.S., Jindal, R., & Kapoor, G. S. (2013). Enzyme-based green approach for the synthesis of *Gum tragacanth* and arylic acid crosslinked superabsorbent-its utilization in controlled fertilizer release and enhancement of water holding capacity of soil. *Iranian Polymer Journal*, 22, 561-570.
20. Saruchi, Kaith, B.S., Jindal, R., Kapur, G.S. & Kumar, V. (2014). Synthesis, characterization and evaluation of Gum tragacanth and acrylic acid hydrogel for sustained calcium chloride release-enhancement of water holding capacity of soil. *Journal of the Chinese Advanced Materials Society*, 2, 40-52.
21. Ma, C., & Prabhu S. (2011). Characterization of a novel lyophilized chitosan hydrogel complex for the controlled release of a highly water soluble drug, niacinamide. *Journal of Drug Delivery***,** 3**,** 55-63.
22. Miller, D. A., Dinunzio, J. C., Yang, W., Mcginity J. W., & Williams, R.O. (2008). Targeted intestinal delivery of supersaturated itraconazole for improved oral application. *Pharmaceutical Research***,** 25**,** 1450-1459.
23. Peppas, N. A., & Ende, D. J. A. (1997). Controlled release of perfumes from polymers. II. Incrporation and essential release of essential oils from glassy polymers. *Journal of Applied Polymer Science* **,** 66, 509-513.
24. Lohani A., Singh G., Bhattacharya SS., & Verma A. (2014). Interpenetrating Polymer Networks as Innovative Drug Delivery Systems. *Journal of Drug Delivery*, http://dx.doi.org/10.1155/2014/583612

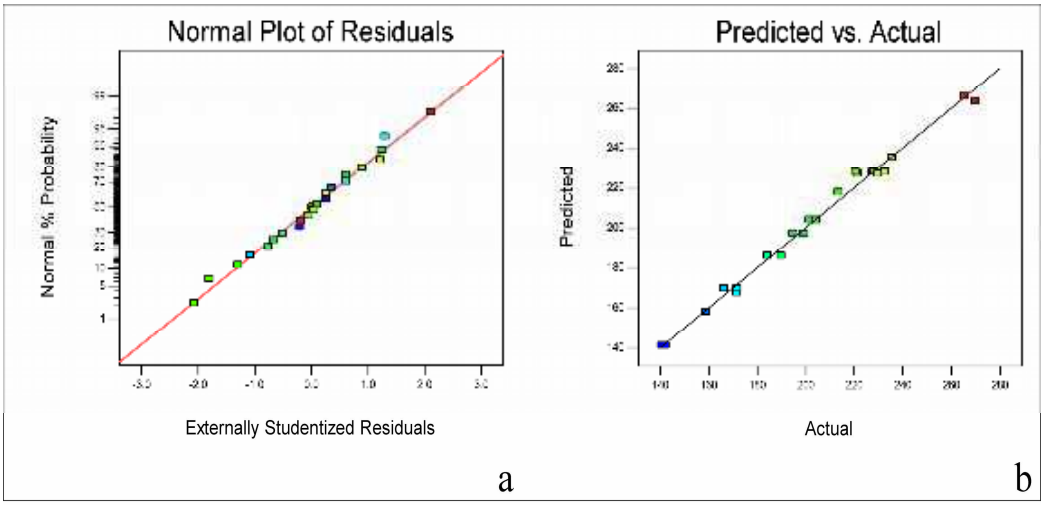

Fig. 1

Fig.1 a) Normal plot of residual b) Actual vs. predicted plot for percentage swelling

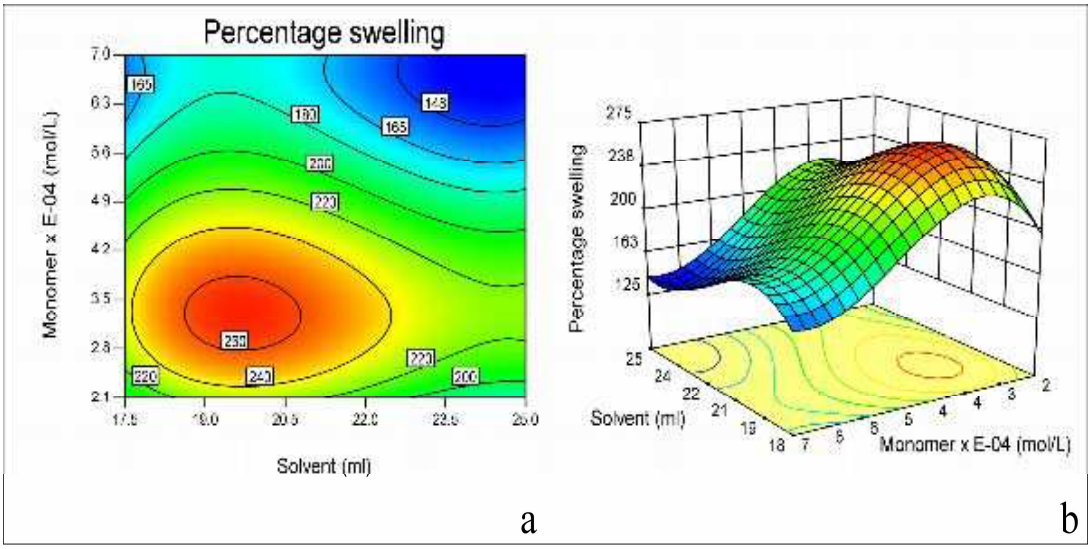

Fig. 2

Fig.2 a) 2-D b) 3-D contour plot showing percentage swelling *vs.* solvent and monomer concentration

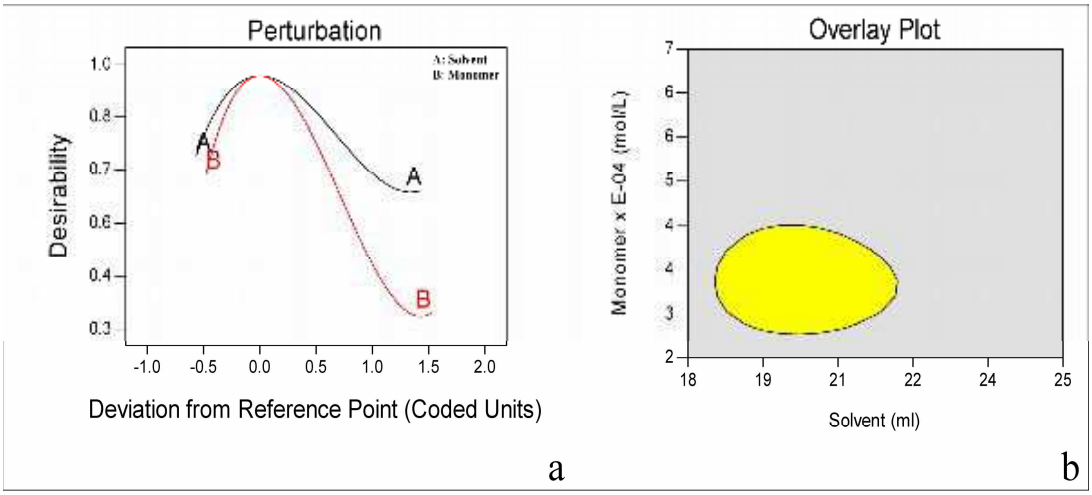

Fig. 3

Fig.3 a) Perturbation plot showing response sensitivity using desirability function b) Overlay plot for achieving minimum percentage swelling of 250.

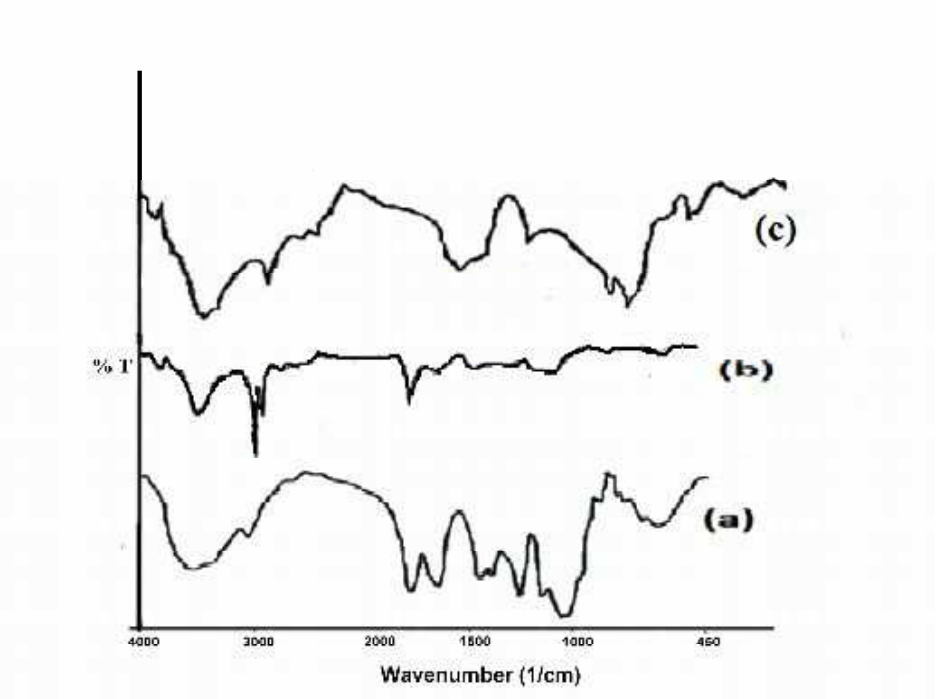

Fig.4

Fig. 4 FT-IR spectrum of (a) Gum tragacanth, (b) Gt-cl-poly(AA) and (c) Gt-cl-poly(AA-ip-AAm)

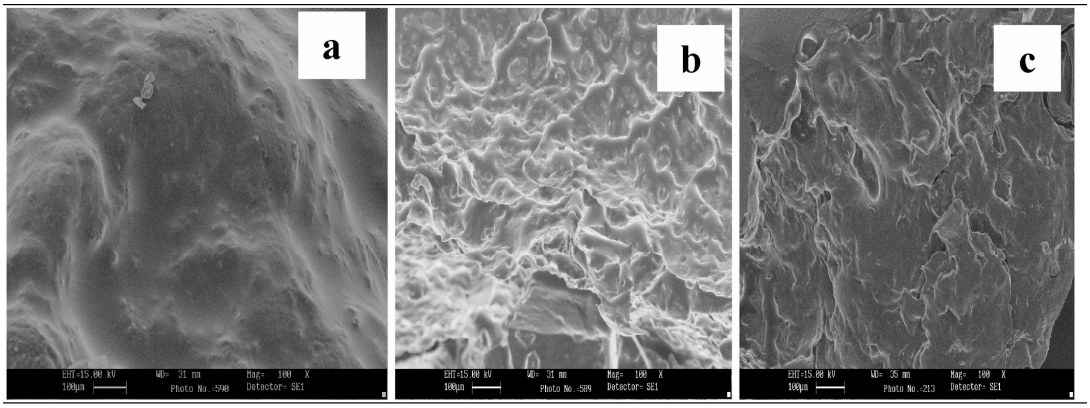

Fig.5$_{a-c}$ SEM of (a*) Gum tragacanth*, (b) Gt-cl-poly(AA) and (c) Gt-cl-poly(AA-ip-AAm)

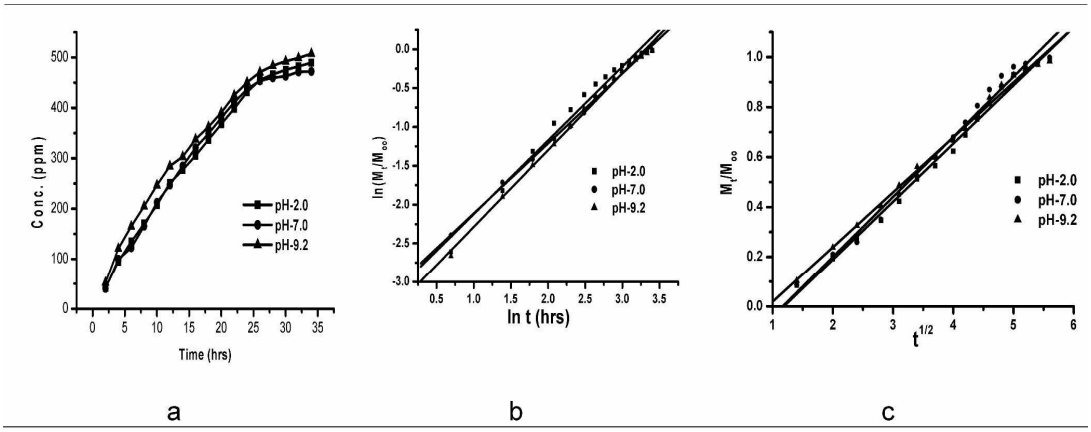

Fig.6$_{a-c}$ Effect of pH onto losartan potassium release behavior through Gt-cl-poly(AA-ip-AAm), (a) conc. vs time, (b) lnM_t/M_∞ vs lnt and (c) M_t/M_∞ vs $t^{1/2}$.

Fig.6 Effect of pH onto losartan potassium release behavior through Gt-cl-poly(AA-ip-AAm), (a) Conc. *vs.* time, (b) ln M_t/M_{oo} *vs.* lnt and (c) M_t/M_{oo} *vs.* $t^{1/2}$

Table 1: Design summary for IV-optimal response surface

Factor	*Name*	*Units*	**Minimum**	**Maximum**
			Actual (Coded)	
A	Solvent	ml	17.5 (-1)	25 (+1)
B	Monomer x E-04	mol/L	2.11 (-1)	7 (+1)
Response variable			Actual	
Ps	Percentage swelling	%	140.6	270.0

Table 2: Optimal response surface design with coded and actual values with percentage swelling

	Factor 1	Factor 2	Factor 1	Factor 2	Response	
Std	Solvent	Monomer	Solvent (ml)	Monomer x 10^{-4} (mol/L)	Percentage swelling	
	Coded values		*Actual values*		Actual	Predicted
1	-1.00	-1.00	17.50	2.11	194.9	197.3
2	-1.00	-1.00	17.50	2.11	199.3	197.3
3	-0.20	-1.00	20.50	2.11	221.4	226.9
4	1.00	-1.00	25.00	2.11	184.2	185.9
5	1.00	-1.00	25.00	2.11	189.8	185.9
6	0.40	-0.63	22.75	3.01	235.7	235.3
7	-0.56	-0.42	19.15	3.53	270.0	263.5
8	1.00	-0.28	25.00	3.87	213.5	217.7
9	0.00	0.00	21.25	4.56	227.6	227.8
10	0.00	0.00	21.25	4.56	220.4	227.8
11	0.00	0.00	21.25	4.56	232.6	227.8
12	0.00	0.00	21.25	4.56	228.0	227.8
13	-1.00	0.11	17.50	4.81	201.6	204.0
14	-1.00	0.11	17.50	4.81	204.4	204.0
15	0.66	0.36	23.73	5.44	171.7	167.7
16	-1.00	1.00	17.50	7.00	158.9	158.1
17	-0.10	1.00	20.88	7.00	166.2	169.7
18	-0.10	1.00	20.88	7.00	171.7	169.7
19	1.00	1.00	25.00	7.00	140.6	141.3
20	-0.44	-0.52	19.60	3.29	265.2	265.9
21	-0.20	-1.00	20.50	2.11	229.8	226.9
22	1.00	1.00	25.00	7.00	142.1	141.3

Table 3: ANOVA table for reduced cubic model

Source	Sum of Squares	df	Mean Square	F-Value	p-value Prob > F
Model	26234	8	3279	173.9	< 0.0001*
A-Solvent	811	1	811	43.0	< 0.0001*
B-Monomer	3254	1	3254	172.6	< 0.0001*
A x B	12	1	12	0.7	0.4334 #
A^2	1950	1	1950	103.4	< 0.0001*
B^2	4662	1	4662	247.3	< 0.0001*
A^2B	95	1	95	5.0	0.0431*
A^3	499	1	499	26.4	0.0002*
B^3	1446	1	1446	76.7	< 0.0001*
Lack of Fit	88	4	22	1.3	0.3550 #
Model statistics					
Std. Dev.	4.34		R^2	0.991	
Mean	203.2		Adj R^2	0.985	
C.V. %	2.14		Pred R^2	0.976	
PRESS	630		Adeq Precision	44.9	

* significant at p<0.05
# not-significant at p<0.05